Journal of Alloys and Compounds 499 (2010) 53–56

Contents lists available at ScienceDirect

Journal of Alloys and Compounds

journal homepage: www.elsevier.com/locate/jallcom

A novel red-emitting phosphor for white light-emitting diodes

Fuqiang Ren, Donghua Chen*

Key Laboratory of Catalysis and Material Science of the State Ethnic Affairs Commission & Ministry of Education, College of Chemistry and Material Science, South Central University for Nationalities, Wuhan 430074, Hubei, PR China

ARTICLE INFO

Article history:
Received 19 November 2009
Received in revised form 7 January 2010
Accepted 9 January 2010
Available online 18 January 2010

Keywords:
Luminescence
Solid-state reaction
UV-LEDs
Nanomaterials

ABSTRACT

A novel red-emitting phosphor of Eu^{3+}-activated molybdate was prepared at 850 °C by a modified solid-state reaction. Photoluminescence (PL) results showed that the phosphor can be efficiently excited by UV–visible light from 350 to 550 nm, and exhibited bright red emission at 614 nm. XPS are taken to investigate the structure and compositions of this material. The crystallization and particle sizes of the phosphor have been investigated by using powder X-ray diffraction (XRD) and transmission electron microscopy (TEM). TEM images show that the grain size of the phosphor is about 30 nm which is in full agreement with the theoretical calculation data from the XRD patterns.

1. Introduction

White light-emitting diodes (LEDs) offer benefits such as stability, energy saving, perpetuation and safety so that they are receiving much attention [1]. They have a great number of important applications in backlight of the liquid crystal display (LCD), automobile light and traffic signals, etc. [2].

In recent years, the studies on tricolor phosphors suitable for near-ultraviolet (UV) excitation have been attracting more attention for fabricating WLED with n-UV chip for white lighting. The presently used phosphors for near-UV/violet GaN-based LED are $BaMgAl_{10}O_{17}:Eu^{2+}$ for blue and $Y_2O_2S:Eu^{3+}$ for red, respectively. However, these sulfide-based phosphors are chemically unstable and the lifetimes of these materials are inadequate, and their luminescent intensities are very low relative to blue and green phosphors [3]. Therefore, the search for a stable, inorganic rare-earth-based red phosphors with high absorption in the near-UV/blue spectral region is an attractive research task. However, only a few red inorganic fluorescence compounds $Y_2O_2S:Sm^{3+}$ [4], $Y_3Al_5O_{12}:Eu^{3+}$ [5] and $Y_2O_2S:Eu^{3+},Si^{4+},Zn^{2+}$ [6], have been reported to the efficient red component with application in UV-LED. Molybdates [7,8] and tungstates [9] with scheelite structure are considered as good host lattice under near-UV or blue excitation due to its MoO_4 tetrahedron unit. Two types of compounds, exemplified by $Sc_2(WO_4)_3$ and $Gd_2(MoO_4)_3$, have been studied by single crystal X-ray diffraction and the unit cell determined. The former is orthorhombic and the latter is tetragonal [10]. Nassau et al. gave a survey of the structures of tungstates and molybdates with the formula $RE_2(WO_4)_3$ along the rare-earth series [11]. These materials have broad and intense charge transfer (CT) absorption bands in the UV and therefore capable of efficiently capturing the emission from a GaN-based LED over a range of wavelength.

Charge compensation plays an important role in improving the luminescence efficiency of phosphors. It has been reported that a charge-compensated phosphor is brighter than that of uncompensated phosphors [12–14]. Cl^- co-doping helps to incorporate Eu^{3+} into lattice sites by increasing the crystallinity. In our present work, using urea and polyethylene glycol (PEG) as auxiliary reagents, ammonium chloride as charge compensation agent, the novel red-emitting phosphor Eu^{3+}-activated molybdate has been successfully synthesized by the modified solid-state reaction. Under near-UV excitation, Eu^{3+}-activated molybdate phosphor emitted an intense red light. Characterization of the powders was carried out by using powder X-ray diffraction (XRD) and transmission electron microscopy (TEM).

2. Experimental procedures

2.1. Sample synthesis

Powder samples with the general composition $(La,Gd)_2(MoO_4)_3$ (LGM) and $(La,Gd)_2(MoO_4)_3{\cdot}xEu_2O_3$ ($x = 0.005–0.05$) (LGME) were prepared at 850 °C by a modified solid-state reaction. The starting materials obtained from Sinopharm Chemical Reagent Co., Ltd., were Eu_2O_3 (4N), La_2O_3 (4N), Gd_2O_3 (3.5N), $(NH_4)_6Mo_7O_{24}{\cdot}4H_2O$ (AR), NH_2CONH_2 (AR), NH_4Cl(AR), polyethylene glycol (PEG) with an average molecular weight of M_n: 3500–4500 g mol^{-1} (AR). Eu_2O_3 was dissolved in HNO_3 solution and Exactly quantified $(NH_4)_6Mo_7O_{24}{\cdot}4H_2O$, La_2O_3, Gd_2O_3, NH_4Cl, $CO(NH_2)_2$ and PEG were sufficiently ground in agate mortar at room temperature. Then nitrates solution was introduced and the mixture was carefully ground in agate mortar at

* Corresponding author. Tel.: +86 27 67841856; fax: +86 27 67842752.
E-mail address: chendh46@hotmail.com (D. Chen).

0925-8388/$ – see front matter © 2010 Elsevier B.V. All rights reserved.
doi:10.1016/j.jallcom.2010.01.039

room temperature for about 10 min. Subsequently the white sol was dried in a thermostatic oven at 100 °C for about 10 min, and an opalescent precursor was attained. The opalescent precursor was transferred to a muffle furnace preheated to 600 °C, with boiling, the solution evaporated and gave out a great lot of smoke and the entire process lasted for 3–5 min, the black precursor was obtained. Finally the black precursor was devolved to a muffle furnace preheated to 850 °C and kept for 4 h, then white phosphor powders (LGME) were obtained. The conventional solid-state reaction for preparing phosphors requires a high calcining temperature generic above 1200 °C. In this paper, using urea and the PEG as auxiliary reagents the red phosphor (LGME) has been successfully synthesized just at 850 °C by this method (the modified solid-state reaction). By this method we had successfully synthesized $(Sr_{0.85}Zn_{0.15})_3(PO_4)_2:Eu^{3+}$ [15].

2.2. Sample characterization

The thermal behaviour of the opalescent precursor was studied by thermogravimetric (TG) analysis using a TGS-2 thermal balance (Perkin-Elmer Co., USA). The XPS patterns of the products were measured by an X-ray photoelectron spectrometer (Thermo VG Multi Lab2000 America) using a monochromic Al K_α light source. Each spectrum was calibrated using the C1s binding energy at 284.63 eV. The synthesized powders were identified by X-ray powder diffractometer (XRD; Bruker D8, Germany), operating at 40 kV and 40 mA and using Cu K_α radiation ($\lambda = 1.5406$ Å). The XRD patterns were collected in the range of $5^\circ \leq 2\theta \leq 120^\circ$. A step size of 0.02° ($2\theta$) was used with scanning speed of 4°/min. The morphology and dimension of the product were observed by transmission electron microscope (TEM), which were taken on a Tecnai G20 (FEI Corporation of Holland) transmission electron microscopy using an accelerating voltage of 200 kV. The emission spectrum was performed by using a Perkin-Elmer LS-55 (Perkin-Elmer Corporation, USA) luminescence spectrophotometer equipped with a xenon discharge lamp as an excitation source. All the luminescent properties of the phosphors were studied at room temperature.

3. Results and discussion

3.1. Structure and phase characterization

The TG/DTG curves of the opalescent precursor of $(La,Gd)_2(MoO_4)_3{\cdot}xEu_2O_3$ ($x = 0.03$) obtained by heating the precursor in air at a heating rate of 10 °C min^{-1} are presented in Fig. 1. There are three main stages of weight loss. The initial weight loss (25%) observed in the TG curve between 120 and 180 °C results from desorption of the adsorbed moisture. At the temperature range 180–240 °C, the main loss (46%) corresponds to the decomposition of urea, ammonium chloride and ammonium nitrate coming from $(NH_4)_6Mo_7O_{24}$ and nitrates. The third weight loss step occurred between 240 and 700 °C, which was attributed to the burning of the PEG ligand and the decomposition of metal nitric. From 700 to 800 °C the weight loss little by little, thereafter, the weight loss remains constant, which indicates that the decomposition and combustion of all organic materials components in the precursor have been completed below 800 °C.

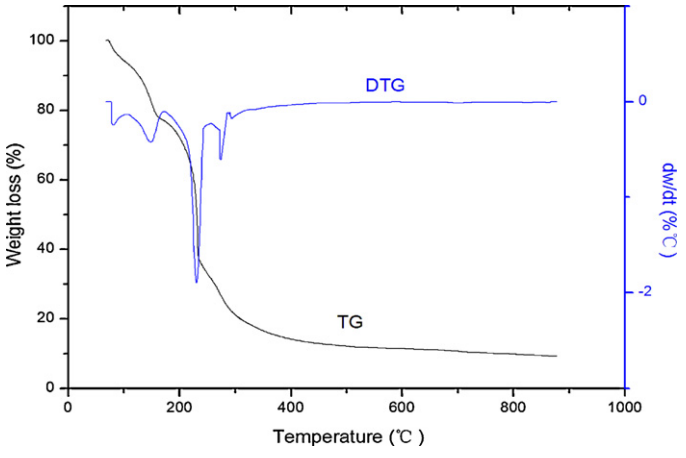

Fig. 1. TG/DTG curves of the thermal decomposition of the opalescent precursor at the heating rate of 10 °C min^{-1} in air.

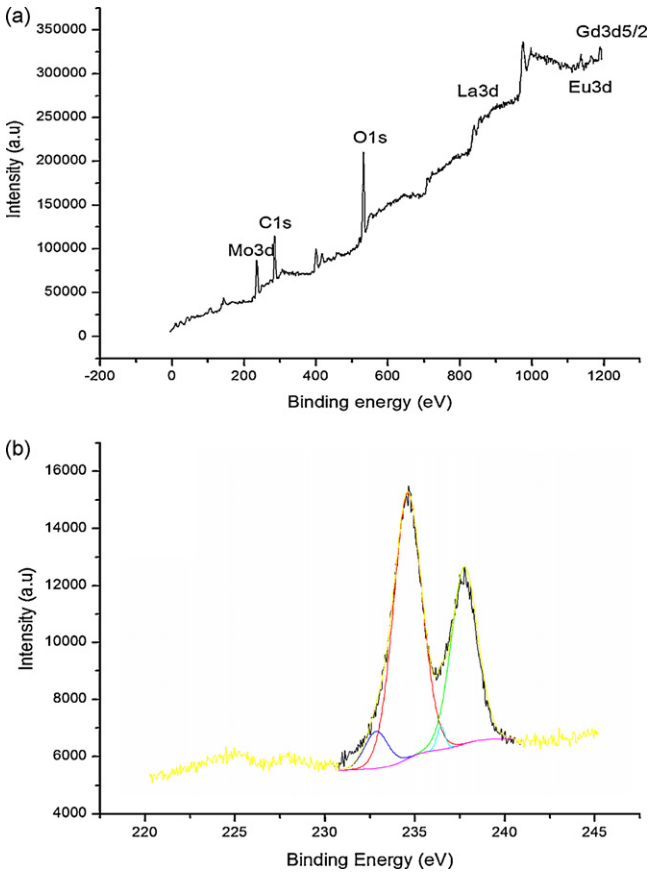

Fig. 2. XPS survey spectra of the LGME.

The general theoretical weight loss calculated from the ratios of starting materials is in good agreement with TG result.

X-ray photoelectron spectroscopy (XPS) was used to investigated the chemical analysis and atom state of the phosphor surface. Fig. 2 reports the XPS survey spectra of the $(La,Gd)_2(MoO_4)_3{\cdot}xEu_2O_3$ ($x = 0.03$). XPS depth profiling studies revealed the existence of Mo, La, Gd, O and Eu atoms. Taking into account the atomic concentration of O, Mo, Gd, La and Eu atoms, results for LGME sample lead to the following relative concentrations: O (82.19%), Mo (12.45%), Gd (1.38), La (2.68) and Eu (1.3%). The samples gave peaks 532.26 eV in the O1s region, 1188.6 eV in the $Gd3d_{5/2}$ region, 836.4 eV in the La3d region and 1136.22 eV in the Eu3d region (Fig. 2a). To verify the oxidation states of the molybdenum centers, XPS experiments were collected and confirmed the mixed valent nature of the element. Upon curve fitting, the XPS plot contains four bands: Mo^{5+} $3d_{5/2}$ (232.85 eV), Mo^{6+} $3d_{5/2}$ (234.60 eV), Mo^{5+} $3d_{3/2}$ (236.45 eV) and Mo^{6+} $3d_{3/2}$ (237.75 eV) (Fig. 2b). These values are in agreement with the values found in the literature ($3d_{5/2}$ BE = 231.10 eV for Mo^{+5} and $3d_{5/2}$ BE = 232.50 eV for Mo^{+6} with $3d_{3/2}$ contributions at +3.13 eV) [16]. Therefore, the LGME is a complex compound containing O, Gd, Eu, La and with the +5 and +6 valence state of molybdenum.

The X-ray diffraction patterns of $(La,Gd)_2(MoO_4)_3{\cdot}xEu_2O_3$ ($x = 1$–5%) are shown in Fig. 3. For the obtained phase, it is carefully observed that there are no peaks of raw materials. It is found that the main phase does not agree with any JCPDS available. The XRD patterns of samples with various Eu^{3+} concentrations (1–5%) have been measured. Fig. 4 shows the XRD patterns of the $(La,Gd)_2(MoO_4)_3{\cdot}xEu_2O_3$ ($x = 0.03$) at different temperatures, the intensity of the peaks of LGME at 1000 °C is little infirmer than the peaks at 850 °C. The results show that different Eu^{3+} concentra-

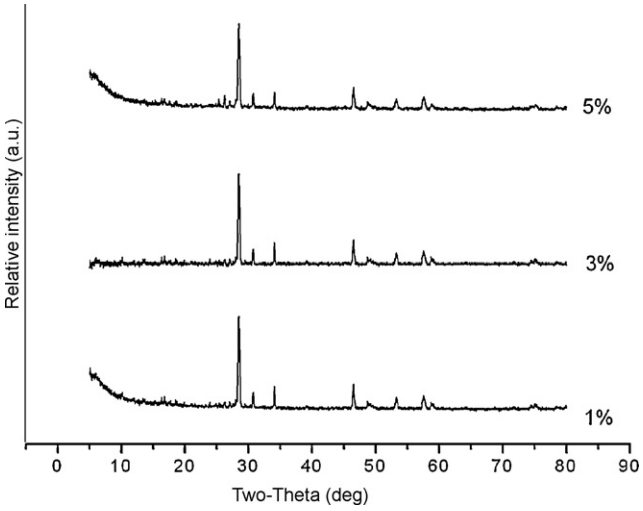

Fig. 3. XRD pattern of LGME phosphor sample.

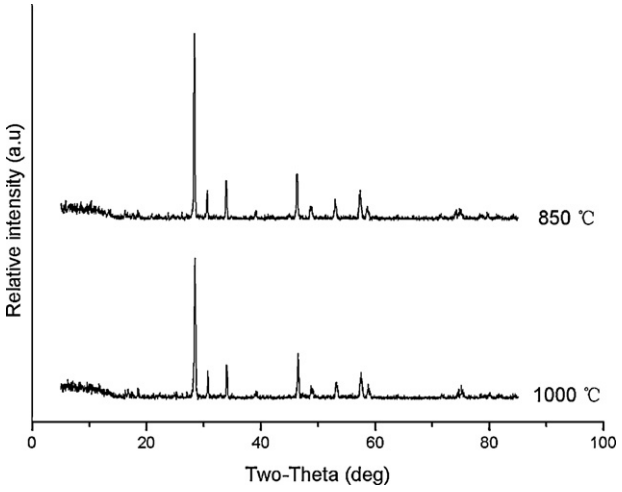

Fig. 4. XRD patterns of the samples at different temperatures.

tions and different temperatures do not result in new other phase except the unknown main phase. Consequently, we speculate that the obtained unknown phase is likely to be a new phase. With respect to this point, a further study is still being carried on.

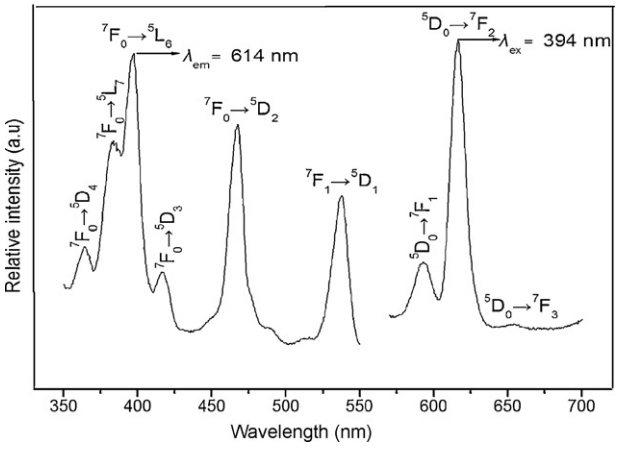

Fig. 6. Excitation and emission spectra of LGME phosphor (the Eu^{3+} concentration is 3 mol%, λ_{em} = 614 nm and λ_{ex} = 394 nm).

The average structural unit distance was estimated from the full width at half maximum of the diffraction peak by the Sherrer equation [17]:

$$D = \frac{k\lambda}{B\cos\theta}$$

where D is the mean crystallite diameter, k (0.89) is the Scherrer constant, λ is the X-ray wave length (1.5406 Å), and B is the full width half maximum (FWHM) of LGME diffraction peak. The average crystallite sizes calculated using the most intense reflection at $2\theta = 28.48^\circ$ are 30.1 nm. The morphologies of $(La,Gd)_2(MoO_4)_3{\cdot}xEu_2O_3$ ($x = 0.03$) nanoparticles are clearly demonstrated by TEM image, as shown in Fig. 5. The LGME phosphor particles exhibited no aggregation and had regular morphology characteristics without any visible admixture of any impurity phases. The grain size of the sample is about 30 nm which is in full agreement with the data from the XRD patterns.

3.2. Luminescence properties

Fig. 6 presents the emission and excitation spectra of the $(La,Gd)_2(MoO_4)_3{\cdot}xEu_2O_3$ ($x = 0.03$). Upon excitation with 394 nm UV irradiation, the emission spectra are described by the well-known $^5D_0 \rightarrow {}^7F_J$ ($J = 1, 2, 3$) emission lines of the Eu^{3+} ions with the strong emission for $J = 2$ at 614 nm, which allows that the Eu^{3+} occupies a center of asymmetry in the host lattice [18]. It is well known

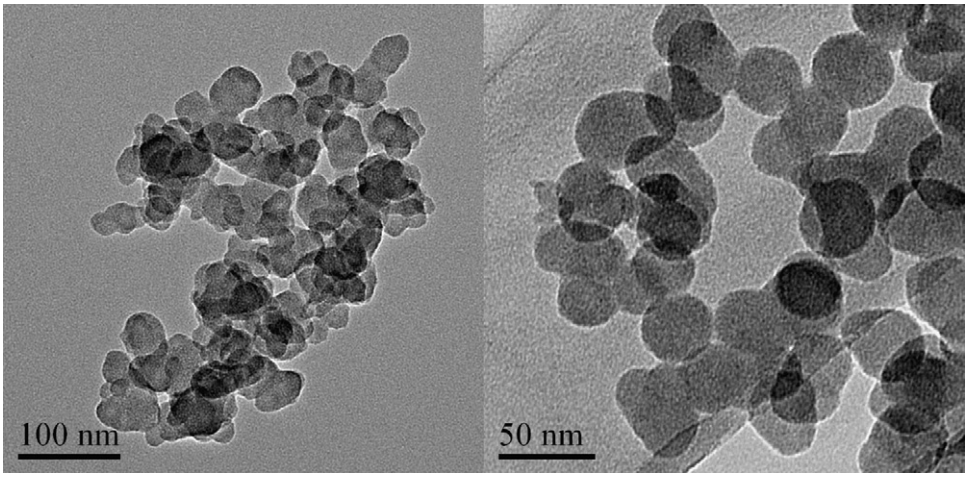

Fig. 5. TEM images of the LGME with 100 and 50 nm.

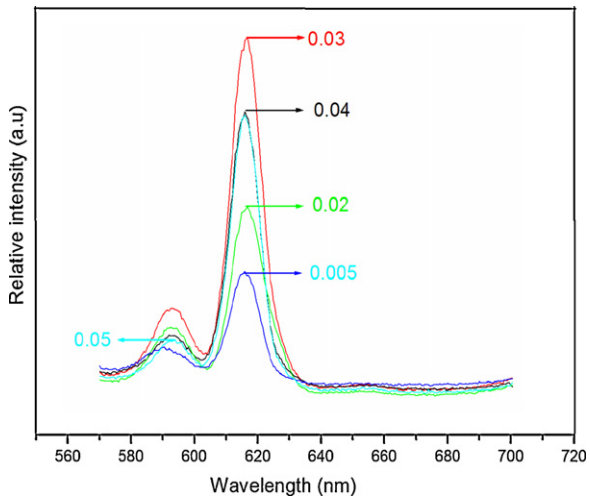

Fig. 7. The emission spectra of LGME phosphor with varying Eu^{3+} concentrations (the mole ratio of the Eu^{3+} is 0.005, 0.02, 0.03, 0.04, 0.05) (λ_{ex} = 394 nm).

that the $^5D_0 \rightarrow {}^7F_2$ red emission of Eu^{3+} ions belong to hypersensitive transitions with J = 2, which is strongly influenced by the outside surroundings and can be served as a very efficient and sensitive structural probe [19–21]. When Eu^{3+} ions are located at high symmetry local sites (with inversion symmetry center) [19,22], the $^5D_0 \rightarrow {}^7F_2$ emission is usually weaker than the $^5D_0 \rightarrow {}^7F_1$ emission in the spectrum. Obviously, the Eu^{3+} ions are located at low symmetry local sites in the host lattice. Based on their close ionic radii [$r(Eu^{3+})$ = 1.087 Å, $r(Gd^{3+})$ = 1.078 Å] and valence state (3+) in LGME, the doped Eu^{3+} ions prefer to occupy the Gd^{3+} sites [23]. Other transitions from the $^5D_0$ excited levels to ^7F_J ground states in the 570–700 nm range are relatively weak. There are no observed differences for the emission band shape and position under different excitation wavelength (λ_{ex} = 362, 384, 412, 464 and 533 nm) except for luminescent intensity. The sharp peaks above 350 nm are due to the intra-configurational (f–f) transitions of Eu^{3+}, including the peaks with maxima at 362 nm ($^7F_0 \rightarrow {}^5D_4$), 384 nm ($^7F_0 \rightarrow {}^5L_7$), 394 nm ($^7F_0 \rightarrow {}^5L_6$), 412 nm ($^7F_0 \rightarrow {}^5D_3$), 464 nm ($^7F_0 \rightarrow {}^5D_2$) and 533 nm ($^7F_1 \rightarrow {}^5D_1$), respectively [24,25]. Among them, the intensity of the peaks at 394 and 464 nm excitation wavelengths (which are emission wavelengths of near-UV and blue LED chips, respectively), is much stronger than the other transitions of Eu^{3+}. This implies that the sample can be effectively excited by radiations of wavelength in the near-UV and blue regions.

The effect of doped-Eu^{3+} concentration on the emission of LGME phosphor was also investigated. The emission spectra of $(La,Gd)_2(MoO_4)_3{\cdot}xEu_2O_3$ phosphors prepared at various concentrations of Eu^{3+} (x = 0.005–0.05) excited by 394 nm are shown in Fig. 7. From Fig. 7, it is observed that with the increase of Eu^{3+} concentration, the intensities of the emission lines are enhanced significantly and reaching a maximum at a concentration of 3 mol% and then decrease due to concentration quenching which is caused by the migration of excitation energy between the emission ions or energy migration to quenching centers where the excitation energy is lost by non-radiative transition.

4. Conclusions

In the present work, the novel red-emitting phosphor, LGME, was prepared by the modified solid-state reaction. TEM images show that the grain size of LGME is about 30 nm which is in full agreement with the theoretical calculation data from the XRD patterns. It is an excellent phosphor for n-UV-LED due to broad excitation band near the UV range and intense emission. It is believed to be a good red phosphor candidate for creating white light in phosphor-converted white LEDs.

Acknowledgment

The financial support from the Key Nature Science Fund of Science and Technology Department of Hubei Province under Grant no. 2001ABA009 for this work is greatly appreciated.

References

[1] F.-b. Caoa, Y.w. Tiana, Y.j. Chenb, J. Alloys Compd. 475 (2009) 387–390.
[2] J.S. Kim, P.E. Jeon, J.C. Choi, H.L. Park, S.I. Mho, G.C. Kim, Appl. Phys. Lett. 84 (2004) 2931.
[3] C.F. Guo, W. Zhang, L. Luan, T. Chen, H. Cheng, D.X. Huang, Sens. Actuators B: Chem. 133 (2008) 33–39.
[4] M. Masuqul Haque, H.-I. Lee, D.-K. Kim, J. Alloys Compd. 481 (2009) 792–796.
[5] C.-H. Lua, W.-T. Hsua, C.-H. Hsua, H.-C. Lub, B.-M. Chengb, J. Alloys Compd. 456 (2008) 57–63.
[6] Z. Huihui, Z. Xinmu, Z. Li, D. Xueping, J. Alloys Compd. 460 (2008) 704–707.
[7] X. Li, Z. Yang, L. Guan, Q. Guo, C. Liu, P. Li, J. Alloys Compd. 464 (2008) 565–568.
[8] X. Yang, X.B. Yu, H. Yang, Y. Guo, Y. Zhou, J. Alloys Compd. 479 (2009) 307–309.
[9] X. Zhang, Z. Li, H. Zhang, S. Ouyang, Z. Zou, J. Alloys Compd. 469 (2009) L6–L9.
[10] K. Nassau, H.J. Levinstein, G.M. Loiacono, J. Phys. Chem. Solids 26 (1965) 1805–1816.
[11] C.A. Kodaira, H.F. Brito, M.C.F.C. Felinto, J. Solid State Chem. 171 (2003) 401–407.
[12] S. Yi, J.S. Bae, K.S. Shim, J.H. Jeong, J.C. Park, P.H. Holloway, Appl. Phys. Lett. 84 (2004) 353.
[13] H. Jang, D. Jeon, Appl. Phys. Lett. 90 (2007) 041906.
[14] S. Chunshan, L. Erbing, J. Alloys Compd. 192 (1993) 40–41.
[15] F.Q. Ren, D.H. Chen, Powder Technol. 194 (2009) 187–191.
[16] C.L. Bianchi, F. Porta, Vacuum 47 (1996) 179.
[17] B.D. Cullity, Elements of X-Ray Diffraction, Addison-Wesley, London, 1978.
[18] S. Shionoya, W.M. Yen, Phosphor Handbook, CRC Press, Boca Raton, FL, 1999, p. 190.
[19] J. Kurian, K.V.O. Nair, P.K. Sajith, A.M. John, J. Koshy, Appl. Superconduct. 6 (1998) 259.
[20] Q. Su, Z. Pei, L. Chi, H. Zhang, F. Zou, J. Alloys Compd. 192 (1993) 25.
[21] J.M. Nedelec, D. Avignant, R. Mahiou, Chem. Mater. 14 (2002) 651.
[22] L.C. Courrol, L. Gomes, A. Brenier, C. Pedrini, C. Madej, G. Boulon, Radiat. Eff. Defects Solids 135 (1995) 81.
[23] G. Blasse, Chemistry and physics of *R*-activated phosphors, in: K.A. Gschneider Jr., L. Eyring (Eds.), Handbook on the Physics and Chemistry of Rare-Earths, North-Holland, Amsterdam, 1979.
[24] S.M. Thomas, P. Prabhakar Rao, K. Ravindran Nair, P. Koshy, J. Am. Ceram. Soc. 91 (2) (2008) 473–475.
[25] J. Wang, X. Jing, C. Yan, J. Lina, J. Electrochem. Soc. 152 (3) (2005) G186–G188.